Kathmandu University
Journal of Science, Engineering and Technology

Simplified design and CFD analysis of Francis turbine components for low-head micro-hydropower applications

Ujwal Makhashya* , Kishor Gurung , Sunil Manandhar , and Neeraj Adhikari

Department of Mechanical and Aerospace Engineering, Pulchowk Campus, Tribhuvan University, Lalitpur, Nepal.

Abstract

This paper presents a simplified design methodology for Francis turbine components for the low-head micro-hydropower applications. The runner is developed using the Bovet method, while the remaining components are designed taking the runner as the reference. For the design of a free vortex-type of spiral casing with circular cross-section, the guidelines provided by UNIDO are considered. Likewise, the guide vanes are modeled using the NACA airfoil profile, and the draft tube adopts a Bend-Spacer-diffuser arrangement to enhance pressure recovery. CFD simulations are performed in ANSYS FLUENT to analyze flow characteristics, pressure distributions, and performance metrics across the distributor, runner, and draft tube. The distributor shows favorable pressure and velocity distributions with a minor head loss of 0.46 m. The runner produces a power output of 17.11 KW with a hydraulic efficiency of 92%, though it operated in off-design conditions, while the draft tube achieves effective pressure recovery despite a major head loss of 1.26 m. The turbine attains an overall efficiency of 83.5%, highlighting the feasibility of a simplified and cost-effective design for small-scale hydropower systems.

Keywords: Francis turbine; Micro-hydropower; Computational fluid dynamics; Bovet method.

1. Introduction

Hydropower is produced in 150 countries worldwide, but Nepal's economically feasible hydropower generation capacity is one of the highest in the world. Nepal, having more than 6000 rivers and rivulets, has one of the highest potentials to become a source of energy security for South Asia [1]. Nepal has a theoretical generation potential of 84,000 MW, out of which 45,610 MW is slated to be techno-economically feasible [2]. According to estimates, Nepal has the potential to generate 40,000 MW from large-scale hydropower and 50 MW from micro-hydro plants. In the case of micro-hydro plants (MHP) in Nepal, Crossflow and Pelton turbines are generally used despite the great potential of Francis turbines. Francis turbines are applicable to a wide range of head and specific speed. Their wide range of applicability, easier manufacturability, and ability to operate efficiently under diverse conditions make them more advantageous than other hydraulic turbines [3]. Owing to this versatility, Francis turbines have become the most widely used turbine type, installed in about 60% of hydropower plants worldwide [4].

The major components of a Francis turbine are the spiral casing, guide vanes, runner, and draft tube. In a hydroelectric turbine system, the spiral casing encases and directs water flow, guide vanes control its velocity, the runner converts water kinetic and pressure energy into mechanical energy, and the draft tube ensures a smooth exit for water, collectively enabling efficient electricity generation from flowing water.

The design and development of Francis turbine components are very technical due to their inherent complexity [5, 6]. Moreover, each requires a unique methodology tailored to specific local design conditions [5, 7]. Nevertheless, many efforts have been made to develop the Francis turbine and its components. In such a process, computational fluid dynamics (CFD) has played a significant role, as it accurately predicts and analyzes three-dimensional flows within the turbomachinery [7, 6].

Several studies have focused on the hydraulic design of Francis turbine components for various head conditions, employing dedicated software tools to generate and analyze turbine geometries [8]. Other works have utilized proprietary design methodology, like Alstom Hydro's approach, for designing large Francis turbines (up to 1000 MW) [9]. Additionally, optimization-based approaches have been proposed, where a preliminary design is derived from different theoretical formulations and later refined through CFD analysis and performance evaluations [7, 6]. A few studies have also integrated structural integrity for the safety of components [10]. These methods show promising results, achieving overall efficiency close to 90% [7, 10]. However, these methods are either difficult to replicate outside highly specialized facilities due to their precision and complexity, or are only suitable for medium to high head applications.

Furthermore, studies depict that the average efficiency of micro-hydropower plants (MHPs) in Nepal is around 59.83%, ranging from 39.7% to 73.5% [12, 13]. This figure is significantly lower than the efficiencies achieved in developed countries [12]. Moreover, most of the MHPs in Nepal are equipped with cross-flow and Pelton turbines [13, 14]. Despite the strong potential of the Francis turbine, it has not yet been adopted in Nepal's MHP sector. More than 3300 plants established to date lack Francis turbine installations, primarily due to insufficient technical expertise in design and manufacturing [5].

To enhance the feasibility and sustainability of Francis turbines for local production, simplified component designs are essential [5, 14]. Several attempts have been made to simplify the Francis turbine for MHP applications. One such approach involved combining guide vanes and stay vanes into a single structure, improving

*Corresponding author. Email: makhashyaujwal@gmail.com

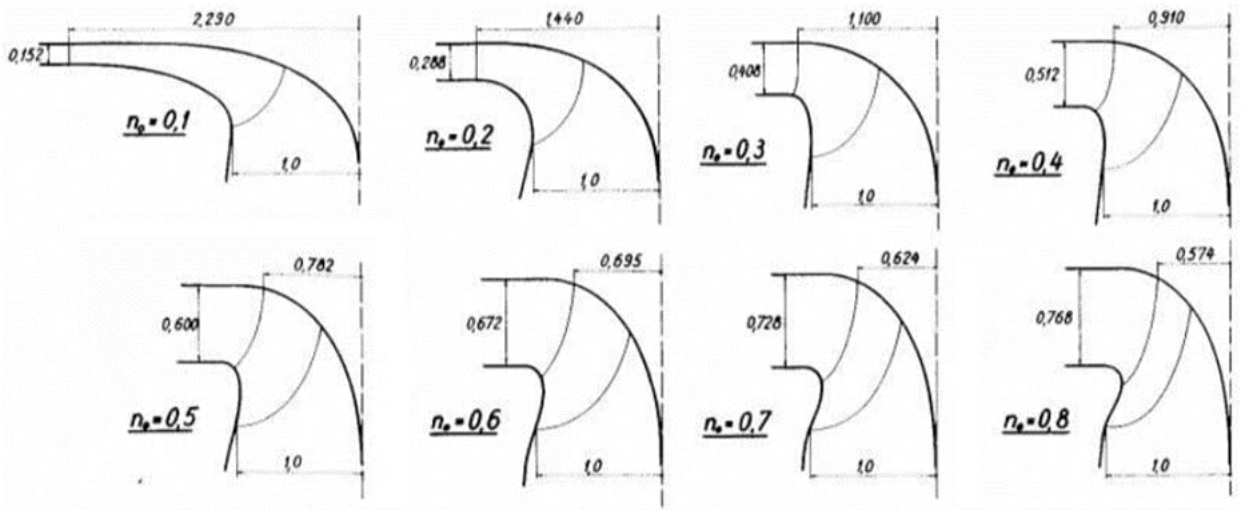

Figure 1: Variation of meridional profile with specific speed [11].

overall efficiency from 86.15% to 90.2% at the Best Efficiency Point (BEP) [5]. Another implemented fixed vanes and a trapezoidal spiral casing, achieving a decent overall efficiency of 82.47% [14], indicating the potential of simplified design in improving efficiencies of MHP performance.

Building upon these previous efforts, the present study aims to develop a generalized and accessible design methodology for Francis turbine components, viz, spiral casing, guide vane, and draft tube for low head applications. In addition, it seeks to perform CFD simulations of the complete turbine to analyze and validate the performance of different turbine components under the head and flow conditions of Damile Micro Hydro Plant located at Pharphing, Kathmandu.

2. Design methodology

The main objective of this study is to design the components of a Francis turbine with dimensions, location, and flow characteristics centered around the runner. The derived runner is developed using the Bovet method and subsequently optimized. The input parameters for the runner, such as head, flow rate, and rotational speed, are the important parameters that govern the design of the turbine components.

For the preliminary design of the spiral casing, in-house MATLAB codes are used, which incorporate different empirical and theoretical formulas, primarily referenced from the Hydrodynamic Design Guide for Small Francis and Propeller Turbines published by the United Nations Industrial Development Organization (UNIDO).

In the case of guide vanes and draft tubes, prior studies are taken into account. The stepwise procedure and theoretical explanations for component designs and CFD analysis are provided in the subsequent chapters. To support the process, a comprehensive list of input parameters used in the initial design is presented in Table 1.

Table 1: Design specification of turbine.

Parameters	Values	Unit
Head, H	15	m
Discharge, Q	0.12	m^3/s

2.1. Design of runner

The Bovet method employs empirical relations to generate the dimension of the meridional profile of a Francis runner. In this approach, the dimensionless specific speed number (n_S) is a critical parameter that governs the profile's shape and geometry. It is evaluated using the equation 1, involving parameters like head (H), flow rate (Q), and rotational speed (N_s) [11, 15].

$$n_0 = \frac{N\sqrt{\frac{Q}{\pi}}}{(2gH)^{3/4}} \tag{1}$$

The hydraulic design of a Francis runner, used as a reference for the development of turbine components, is taken from a previous study [16] and is based on the head and flow conditions of Damile MicroHydro located at Pharphing, Kathmandu.

Various meridional profiles developed using the Bovet method within the operating range $0.1 < n_s < 0.8$ is shown in Fig. 1.

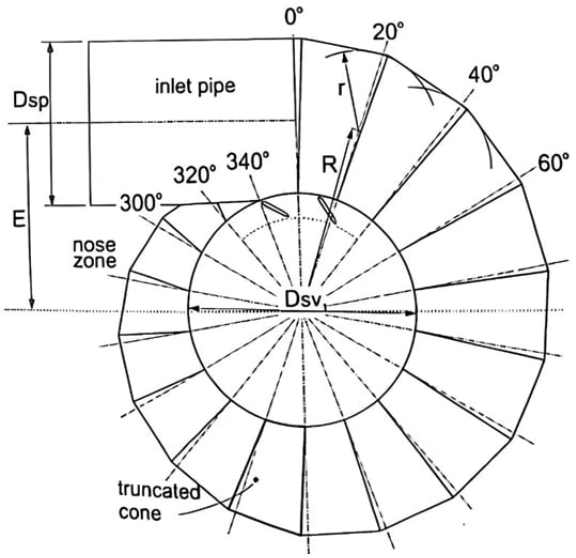

Figure 2: Spiral casing cross plan view [17].

2.2. Design of spiral casing

The primary function of the spiral casing is to deliver a symmetric and uniform flow across the leading edges of the guide vanes. Additionally, it ensures the necessary circulation so that water approaches the guide vanes at an appropriate angle, enabling optimal turbine operation.

A comparative study of spiral casing with square, trapezoidal, and circular cross-sections concluded that, though secondary flow

at the inlet is minimal, it tends to increase as fluid moves further due to the imbalance between radial pressure gradient and centrifugal force [18]. Despite the increase, the circular cross-section has low secondary flow, leading to its selection for the present design.

The free vortex spiral casing was selected from different flow types, including accelerated, decelerated, and free vortex. In the free vortex type, the flow within the guide vanes is nearly axisymmetric, which helps to maintain uniform loading on the runner and minimizes unbalanced forces [19]. Furthermore, it also exhibits lower total pressure losses compared to the accelerated type. Therefore, the design is based on the law of constant velocity moment, which governs free vortex flow distribution.

The spiral casing is designed implementing the guidelines provided in the Hydrodynamic Design for Small Francis and Propeller Turbine by the United Nations Industrial Development Organization (UNIDO) [17].

$$C_{ur} = const. \tag{2}$$

The specific casing entrance velocity (KV_{sp}) is an important parameter to calculate inlet diameter (D_{sp}). It is determined using equation 3.

$$KV_{sp} = -2 \times 10^{-6} n_s^2 + 1.1 \times 10^{-3} n_s + 0.0465 \tag{3}$$

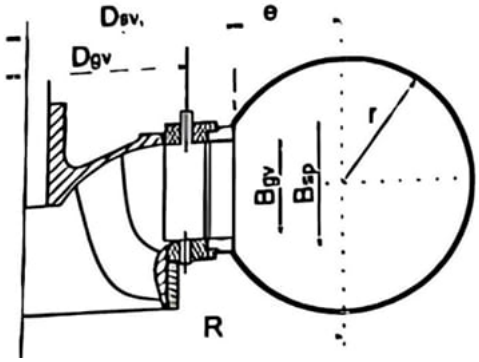

Figure 3: Spiral casing cross section [17].

Likewise, spiral casing inlet diameter (D_{sp}) can be evaluated using equation 4.

$$D_{sp} = \sqrt{\frac{4Q}{\pi KV_{sp}\sqrt{2gH_n}}} \tag{4}$$

Another key parameter, D_{sv}, is determined on the basis of the outer diameter of the guide vane. Similarly, the heights B_{gv} and B_{sp}, as shown in Fig. 3, are evaluated based on the guide vane height.

The cross-sectional area of the spiral casing (A_{Sp}) at various points is calculated using geometric relationship 5.

$$A_{sp} = \pi r^2 - r^2 \arctan(\frac{B_{sp}}{2c}) + \frac{B_{sp}c}{2} \tag{5}$$

where, $B_{sp}$is calculated using equation 6.

$$B_{sp} = 2\sqrt{r^2 - c^2} \tag{6}$$

As shown in the spiral casing cross plane view Fig. 2, non-dimensional area variation with respect to the section angle (θ) is determined using equation 7.

$$\frac{A_{sp\theta}}{A_{sp0^o}} = -0.0028\theta + 1.005 \tag{7}$$

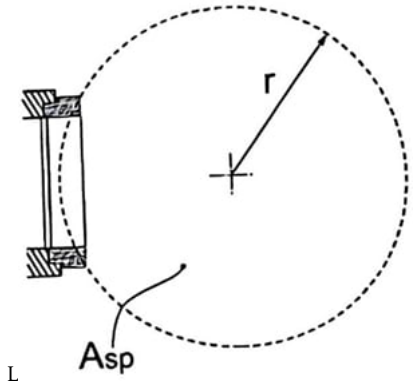

Figure 4: Spiral casing cross section geometry [17].

After evaluating the non-dimensional area variation, the cross-sectional area is computed at 20 equal intervals along the wrap angles, as shown in Fig. 4. These computed cross-sectional areas, plotted in Fig. 5, are used for the design of the spiral casing.

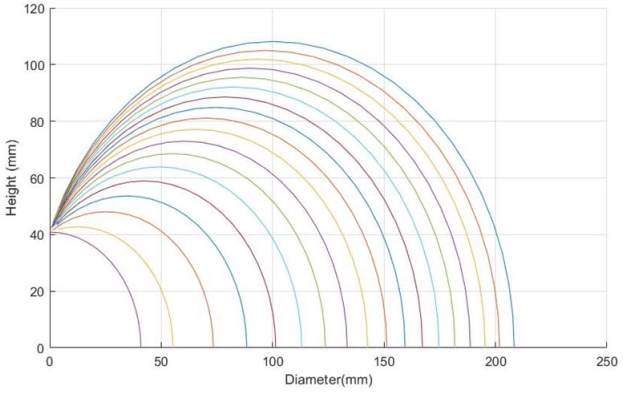

Figure 5: Cross section of spiral casing at different wrap angles.

2.3. Design of guide vanes

The guide vanes redirect the flow around the runner and can be rotated about their axis to regulate water flowing into the runner. Proper placement of the rotation center is essential to avoid the interference between the guide vane blades and the runner blades, particularly when the guide vanes are fully open. Therefore, the diameter of the circle passing through the center of the guide vanes (D_g) is typically set to 1.16 times the runner inlet diameter, as shown in Fig. 7 [17].

The number of guide vanes is selected as 12, based on standard configurations (12, 16, or 24 vanes) that ensure even flow distribution around the circumference while also providing balance and symmetric mechanical design [20].

Once the rotational axis and the number of vanes are determined, their lengths are calculated in such a manner that there is an overlap between the guide vanes when fully closed. The distance between the centers of adjacent guide vanes (t_g), mentioned in Fig. 6, is a key parameter to determine the guide vane length, is approximated as the arc length between two adjacent rotation centers on the guide vane circle. It is calculated using equation 8.

$$t_g \approx \frac{D_g \pi}{number\ of\ guide\ vanes} \tag{8}$$

The mean length of the guide vane (L_g) is designed slightly greater than the pitch distance (t_g) to ensure complete closure. To

achieve a 10% overlap in closed position, the guide vane length L_g is computed using equation 9.

$$L_g = \frac{\pi D_g}{number\ of\ guide\ vanes} \frac{1}{0.9} \tag{9}$$

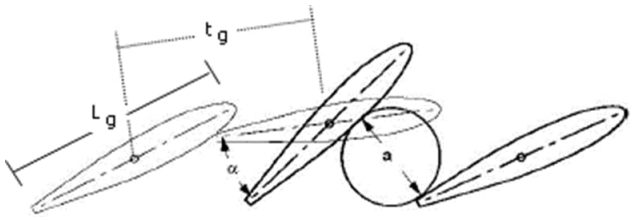

Figure 6: Guide vane dimensions [20].

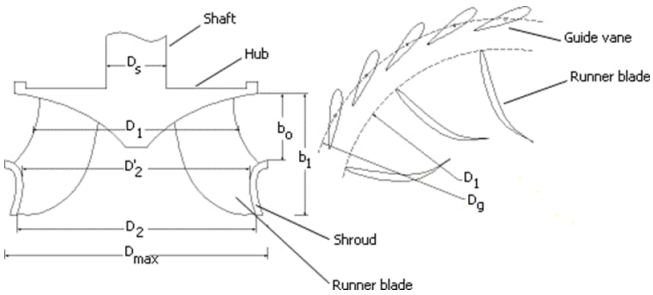

Figure 7: Guide vane location [20].

A guide vane with a symmetric profile offers improved pressure distribution, flow pattern, and also reduces the risk of cavitation [21], which altogether enhances the efficiency and durability of the Francis turbine. Consequently, for the cross-sectional shape, the NACA 0012 airfoil is considered as it is most widely used for guide vanes [22]. Finally, based on numerical calculations, the guide vane angle is determined to be 23 degrees.

2.4. Design of draft tube

The draft tube is a critical component in reaction turbines used primarily for pressure recovery. In addition to recovering pressure, it allows the installation of the turbine above the tailwater level, reduces the exit velocity, and also supports structural design. The arrangement of the draft tube that transfers flow from the outlet of the horizontal turbine to the lower reservoir consists of a Bend-Spacer-Diffuser.

The bend refers to the curved section of the draft tube, which typically follows the outer edge of the turbine and redirects the flow smoothly toward the diffuser section. The spacer is a component installed between the turbine outlet and the beginning of the bend. The diffuser is a final section connected to bend with a gradual increase in diameter from the inlet to the outlet. Its purpose is to decelerate the flow, converting the kinetic energy of water to pressure energy.

Nearly infinite samples of draft tubes can be created by varying the different components of the draft tube, such as a cone, spacer, bend, and diffuser [23].

The performance of the draft tube is highly susceptible to boundary layer development and flow separation, which is mainly influenced by the divergence angle. To mitigate flow separation, the maximum divergence angle is limited to 5 degrees. Additionally, kinetic energy losses at the exit significantly impact the draft tube's hydraulic performance. The exit discharge velocity is kept as low as possible to prevent the effective head loss between 0.2% and 0.5% [24]. However, a decrease in the exit velocity increases the exit area, which could undesirably increase the width of the draft tube outlet. Therefore, the optimum outlet velocity can be determined using equation 10.

$$V_3 = (0.3\ to\ 0.7)\ H_e^{1/2} \tag{10}$$

Where,
V_3 = velocity at draft tube outlet
H_e = effective head of turbine

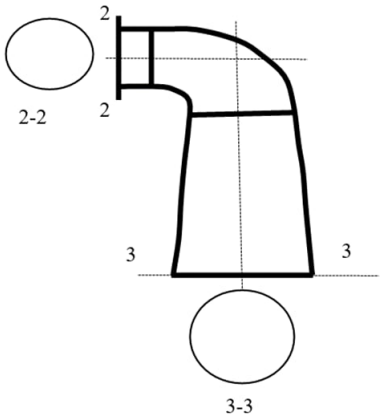

Figure 8: Conical type draft tube [24].

3. Numerical methodology

3.1. Numerical modeling

Numerical analysis is conducted to evaluate the performance of the different components developed for the operation of the Francis turbine runner. To analyze the complex fluid flow within the turbine and its components, computational fluid dynamics (CFD) is employed.

The flow inside the Francis turbine is three-dimensional and turbulent. To accurately capture this, Reynolds-Averaged-Navier-Stokes (RANS) equations are solved using appropriate turbulence models. Furthermore, the complete CFD analysis of the full turbine is carried out in ANSYS FLUENT.

3.2. Geometry generation

The geometry used in the numerical analysis is divided into three components: the distributor, the runner, and the draft tube. The distributor consists of a spiral casing and guide vanes.

In-house MATLAB codes are used to generate dimensions of cross-sections of spiral casing at different wrap angles, based on empirical and theoretical formulations. These sections are then used to construct a detailed 3D model in SolidWorks 2023 and SpaceClaim. In case of guide vanes, NACA 0012 series airfoil is chosen for a cross-section. A total of 12 vanes are arranged in a circular pattern in the calculated position, i.e, guide vane location. Their 3D geometry is also developed in SolidWorks 2023. The runner geometry is generated using the Bladegen and Blade modeler module in ANSYS, incorporating 13 blades as per design specifications. Finally, the draft tube is also developed in SolidWorks using the previously defined Bend-Spacer-Diffuser configuration.

After the generation of solid models, the fluid domain is extracted for each component separately using the volume extraction feature in SpaceClaim. These extracted volumes are then assembled to generate a complete domain for performing CFD simulation.

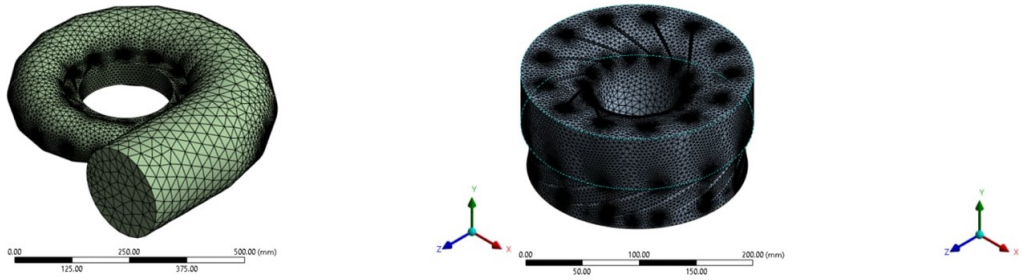

(a) Mesh of spiral casing and guide vanes. **(b)** Mesh of runner.

Figure 9: Meshes used in the study.

3.3. Mesh generation

Meshing is a crucial step in numerical analysis as the structure, quality, and types of mesh have a significant impact on the overall accuracy, computation efficiency, and convergence of the simulation. Hexahedral, tetrahedral, and hybrid meshes are commonly used for CFD analysis. While tetrahedral meshes are easier and faster to generate, hexahedral meshes, being structured, offer superior accuracy, better computational performance, and more efficient memory allocation. In order to make the study and modeling simple and easy, tetrahedral mesh is generated as shown in Fig. 9 and Fig. 10. For the generation, the default mesh generation tool in ANSYS FLUENT is used with a global element size of 30 mm. The mesh size and number are decided via mesh independence test. This configuration resulted, a total of 5288519 elements and 973216 nodes. Table 2 summarizes some of the characteristics of the generated mesh.

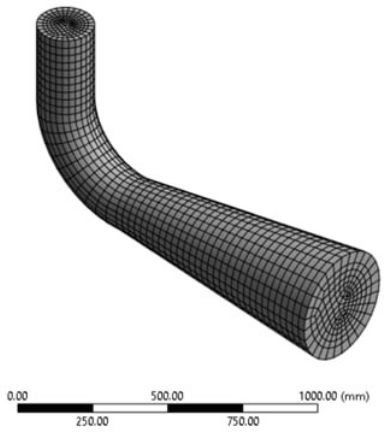

Figure 10: Mesh of draft tube.

Table 2: Mesh specifications.

Parameters	Minimum	Average	Maximum
Skewness	$1.52 * 10^-4$	0.23357	0.97991
Orthogonal Quality	$2.01 * 10^-2$	0.76545	0.99783
0.99783	$2.9 * 10^-2$	0.83405	0.99991
Aspect Ratio	1.8532	64.459	1.07

3.4. Turbulence model

The $k - \omega$ SST model is chosen as a turbulence model for the simulation. The $k - \omega$ SST model blends the perks of both the $k - \epsilon$ model and the $k - \omega$ model, which helps in capturing the wall-bounded and free shear flows. Since most complex turbulence flows include both types of regions, wall-bounded and free shear flows, it is a minimum requirement for a good turbulence model to incorporate both of its use in complex flows. Furthermore, it provides a better prediction of flow separation than most RANS models and accounts for its good behavior in adverse pressure gradients.

3.5. Mesh connections and boundary conditions

A steady-state condition with no-slip viscous boundary conditions is applied at the wall to simulate CFD analysis. The spiral casing, guide vanes, and draft tube are regarded as the stationary domains, whereas a rotational speed of 1500 rpm is assigned to the runner using the Multiple Reference Frame (MRF) method. For boundary conditions, a mass flow inlet of 120 kg/s and a static pressure outlet of 1 atm are used. This turbine setup resulted in an approximate differential head of 17.38m across the turbine. For the modification of the differential head, the guide vane opening angle can be adjusted as mentioned in Kristine Gjøsæter's Master's thesis [8].

4. Result and discussion

A three-dimensional representation of the complete Francis turbine assembly, including the spiral casing, guide vanes, runner, and draft tube, is shown in the Fig. 11. The illustration highlights the geometric integration and alignment of individual components within the turbine system. The detailed dimension specifications of each component are summarized in the Table 3.

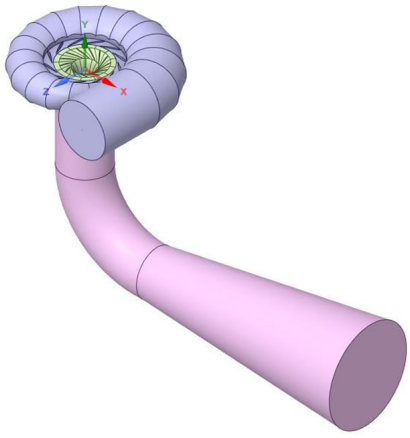

Figure 11: Flow domain of Francis turbine components.

4.1. Distributor

The radial and tangential velocity components at the distributor outlet exhibit a periodic nature, closely aligning with the theoret-

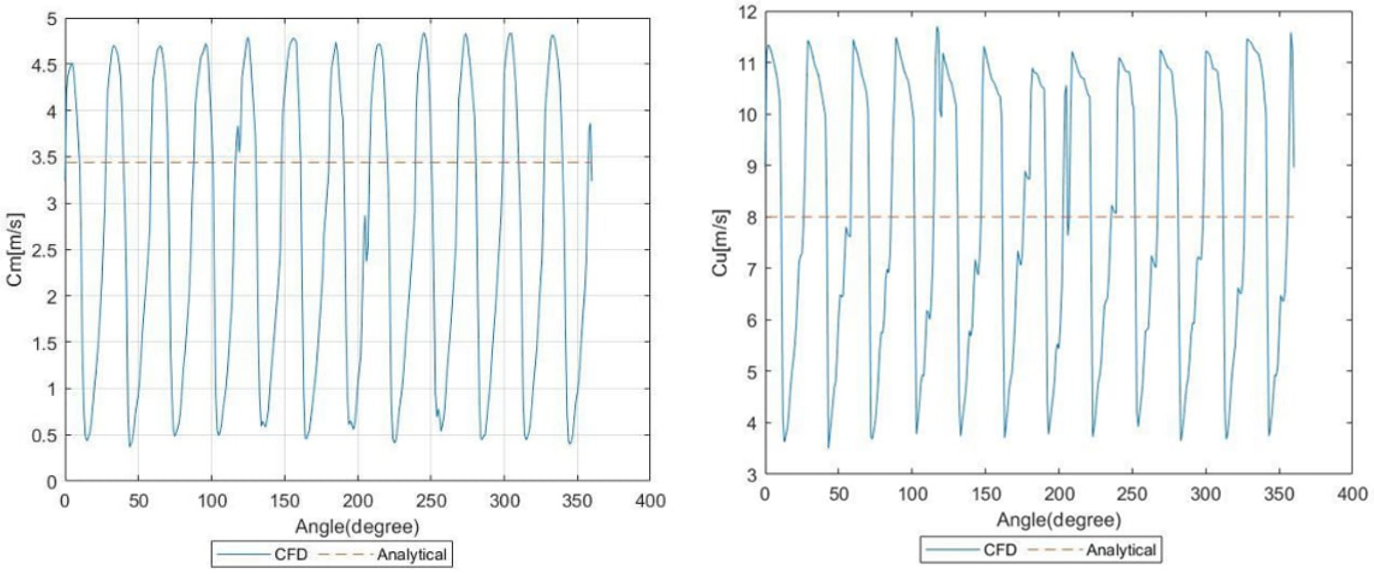

(a) Radial velocity.

(b) Tangential velocity.

Figure 12: Velocity distributions at the guide vane outlet.

Table 3: Component specifications and dimensions.

S.N.	Specifications	Dimensions
1	Spiral Casing	
	a. Inlet diameter	216.39 mm
	b. Outlet diameter	273 mm
2	Guide vanes	
	a. Height	54.12 mm
	b. Length	67.98 mm
	c. Spacing	60.46 mm
	d. Number of blades	12
3	Runner	
	a. Inlet diameter	205 mm
	b. Number of blades	13
4	Draft Tube	
	a. Inlet diameter	194.36 mm
	b. Height	1.2 mm
	c. Outlet diameter	309.6 mm

ical calculation. The fluctuation in the velocity components along the guide vane outlet is due to the position of the guide vanes and runner blades. A portion of the flow exiting the guide vane directly impinges on the runner blades, which leads to a reduction in both tangential and radial velocity components at the guide vane outlet. Furthermore, the plots in Fig. 12 illustrate that the theoretical (analytical) calculations lie within the periodic values.

The pressure contour plot shown in Fig. 13(a) illustrates a uniform pressure distribution, with a gradual decrease in pressure from the spiral casing walls toward its outlet. In contrast, the velocity contour plot shown in Fig. 13(b) illustrates a gradual increase in the flow velocity from the walls to the outlet.

Despite the appealing pressure and velocity contour plots, the entire distributor domain accounts for a head loss of 0.46 m.

4.2. Runner

The design head of the runner is specified as 15 m, and the flow rate is 120 kg/s. However, the CFD simulation of the turbine setup was performed at a net head of 17.38 meters, with the head available to the runner being 15.38 m. Since head and flow rate are interdependent properties, maintaining a constant flow rate can potentially disrupt the other. Kristine Gjøsæter, in their Master's thesis [8] provided a way to change the differential head by changing the guide vane opening angle, which helps in maintaining both head and flow rate. Although it is theoretically possible to carry out a simulation with a 15 m head and a 120 kg/s flow rate. This would require a significant change in the turbine domain. Therefore, the simulation was conducted under off-design conditions.

Despite operating in an off-design condition, the runner produces a torque of 108.93 Nm while operating at 1500 rpm, resulting in a power output of 17.11 KW with a turbine efficiency of 92%, which is within the range [16], and an overall efficiency of 83.59%.

Table 4: Runner parameters when operated at 17.38 m overall head.

Parameters	Preliminary design
Torque	108.93 Nm
Shaft power	17.11 kW

4.3. Draft tube

The draft tube exhibits complex flow dynamics. Fig. 14 illustrates the velocity vectors on the mid-plane of the draft tube. The flow progresses smoothly from the inlet to the outlet of the draft tube, without any flow separation. A steady reduction in velocity from the inlet to the outlet indicates effective pressure recovery. The performance of the draft tube is evaluated through the pressure recovery factor and an energy loss coefficient. CFD simulation reveals a pressure recovery factor of 0.711068 and an energy loss coefficient to be 1.33856, corresponding to a head loss of 1.26 m.

5. Conclusion

This study presented the design and numerical analysis of Francis turbine components suitable for the low-head micro-hydro application. The runner was designed based on the Bovet Method,

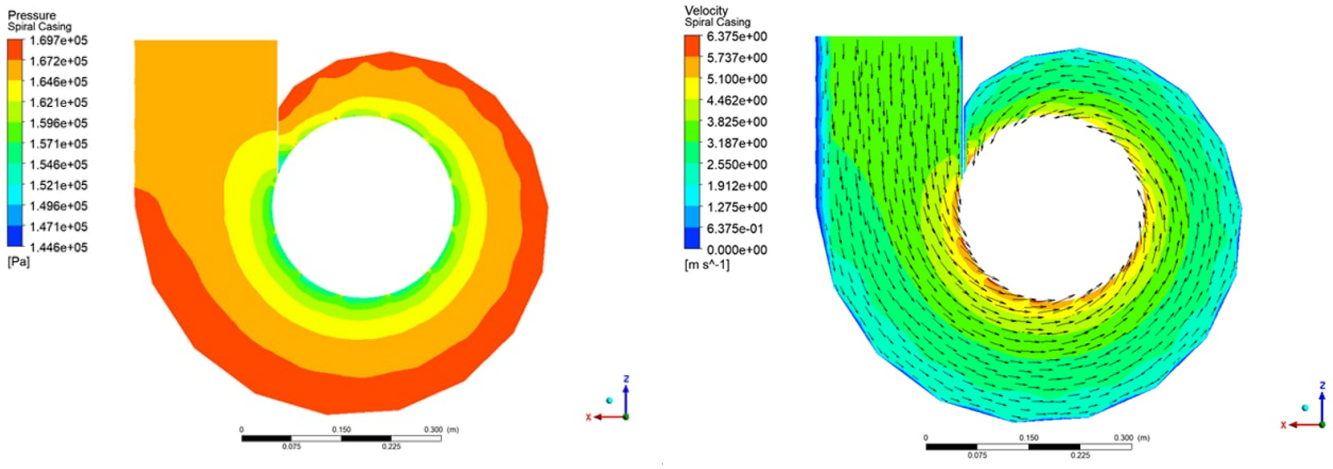

(a) Pressure Contour. **(b)** Velocity Contour.

Figure 13: Contours at the mid plane of the spiral casing.

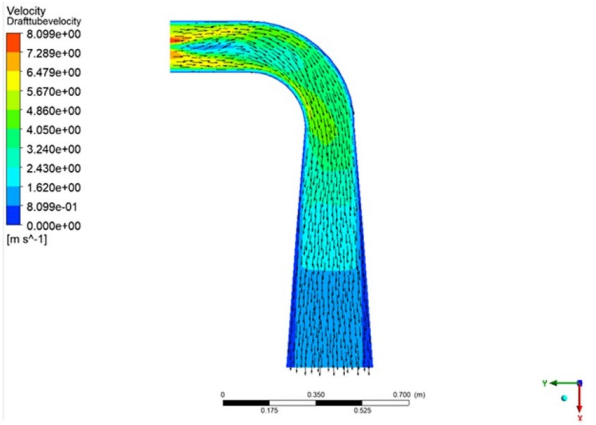

Figure 14: Velocity contour and velocity vector in draft tube.

and other components were generated with reference to the runner. For the design of the spiral casing, design guidelines presented in UNIDO were taken as a reference; guide vanes were modeled with NACA 0012 airfoil profiles, and a Bend-Spacer–Diffuser arrangement was considered for the draft tube. CFD simulation carried out in ANSYS FLUENT provided detailed insights into the hydraulic performance of each component and also of the whole turbine assembly.

The distributor exhibits a uniform velocity and pressure distribution with a head loss of 0.46 m. The runner produces a power output of 17.11 KW with a hydraulic efficiency of 92% despite its operation in off-design conditions. The draft tube also provided a satisfactory performance, showing no flow separations and adequate energy recovery. However, it suffers a major amount of head loss, which is 1.26 m. This loss can be mitigated to some extent by optimizing area ratio and divergence geometry. With an overall efficiency of 83.59%, the turbine demonstrates the possibility of a simplified design to provide a reliable, cost-effective, and manufacturable solution suitable for micro-hydro applications.

The efficiency can be further improved through simple modifications in the draft tube, such as adjusting the bend radius and optimizing the area ratios of the spacer, bend, and diffuser. Furthermore, the incorporation of improved NACA airfoils is expected to increase the efficiency up to 87% under the same off-design conditions. However, this study does not incorporate the Hill Chart, nor is it carried out at the Best Efficiency Point (BEP). Addressing these aspects in future work would provide deeper insights into the feasibility of this study.

Acknowledgment

The University Grant Commission Nepal funded this study with Faculty Research Grant FRG-77/78-Eng-1.

References

[1] Sharma R H & Awal R, Hydropower development in Nepal, *Renewable and Sustainable Energy Reviews*, 21 (2013) 684–693. ISSN 1364-0321. https://doi.org/10.1016/j.rser.2013.01.013.

[2] Agrawal S & Pandey R, Current status of small/micro hydropower in Nepal: A case study of Giringdi SHP, *Journal of the Institute of Engineering*, 15(3) (2019) 21–27. ISSN 1810-3383. https://doi.org/https://doi.org/10.3126/jie.v15i3.31993.

[3] Raabe J. *Hydro power. The design, use, and function of hydromechanical, hydraulic and electrical equipment* (1985). URL https://books.google.com.np/books/about/Hydro_Power.html?id=FOFSAAAAMAAJ&redir_esc=y.

[4] Goyal R & Gandhi B K, Review of hydrodynamics instabilities in Francis turbine during off-design and transient operations, *Renewable Energy*, 116 (2018) 697–709. ISSN 0960-1481. https://doi.org/10.1016/j.renene.2017.10.012.

[5] Dahal D R, Neopane H P, Thapa B S, Paudel N, Chitrakar S & Thapa B, A simplified Francis turbine for micro hydro application: Design and numerical analysis, *IOP Conference Series: Earth and Environmental Science*, 627(1) (2021) 012018. ISSN 1755-1315. https://doi.org/10.1088/1755-1315/627/1/012018.

[6] Patel K, Desai J, Chauhan V & Charnia S, Development of Francis turbine using Computational fluid dynamics (2011) 1–3. https://doi.org/10.13140/2.1.2177.4402.

[7] Akin H, Aytac Z, Ayancik F, Ozkaya E, Arioz E, Celebioglu K & Aradag S, A CFD aided hydraulic turbine design methodology applied to Francis turbines (2013) 694–699. https://doi.org/10.1109/PowerEng.2013.6635694.

[8] Gjøsæter K. *Hydraulic design of Francis turbine exposed to sediment erosion*. Master's thesis, Institutt for energi-og prosessteknikk (2011). URL https://ntnuopen.ntnu.no/ntnu-xmlui/handle/11250/234472?show=full.

[9] Flores E, Bornard L, Tomas L, Liu J & Couston M, Design of large Francis turbine using optimal methods, *IOP Conference Series: Earth and Environmental Science*, 15(2) (2012) 022023. ISSN 1755-1315. https://doi.org/10.1088/1755-1315/15/2/022023.

[10] Celebioglu K, Okyay G & Yildiz M, Design of a Francis turbine for a small hydro power project in Turkey, 49170 (2010) 483–492. https://doi.org/10.1115/ESDA2010-24744.

[11] Kocak E, Karaaslan S, Yucel N & Arundas F, A numerical case study: Bovet approach to design a Francis turbine runner, *Energy Procedia*, 111 (2017) 885–894. ISSN 1876-6102. https://doi.org/10.1016/j.egypro.2017.03.251.

[12] Acharya K & Bajracharya T, Current status of micro-hydro technology in Nepal, 1 (2013) 1. URL https://www.researchgate.net/publication/296348325_Current_Status_of_Micro_Hydro_Technology_in_Nepal.

[13] Khadka S S & Maskey R K, Performance study of micro-hydropower system in Nepal (2012) 265–269. https://doi.org/10.1109/ICSET.2012.6357409.

[14] Ghimire A, Dahal D, Kayastha A, Chitrakar S, Thapa B S & Neopane H P, Design of Francis turbine for micro hydropower applications, *Journal of Physics: Conference Series*, 1608(1) (2020) 012019. ISSN 1742-6596. https://doi.org/10.1088/1742-6596/1608/1/012019.

[15] Karki S, Satyal S, Rijal K, Koirala P & Adhikari N, Comparative CFD analysis of Kali-Gandaki "A" Francis runner with runner generated from Bovet method, *IOP Conference Series: Earth and Environmental Science*, 1037(1) (2022) 012007. https://doi.org/10.1088/1755-1315/1037/1/012007.

[16] Adhikari N, Gurung K, Bajracharya T R & Makhashya U, Determination of the effects of size parameters and lean angle on Bovet-based Francis turbine runner performance, *IOP Conference Series: Earth and Environmental Science*, 1385(1) (2024) 012016. ISSN 1755-1315. https://doi.org/10.1088/1755-1315/1385/1/012016.

[17] Hothersall R, Anestis G & Gürkök C. *Hydrodynamic design guide for small Francis and Propeller turbines*. UNIDO (2004). URL https://downloads.unido.org/ot/47/88/4788275/20001-_23096.pdf.

[18] Dahal D, Chitrakar S, Kapali A, Thapa B & Neopane H, Design of spiral casing of Francis turbine for micro hydro applications, *Journal of Physics: Conference Series*, 1266(1) (2019) 012013. ISSN 1742-6596. https://doi.org/10.1088/1742-6596/1266/1/012013.

[19] Kurokawa J & Nagahara H, Flow characteristics in spiral casings of water turbines, *TRANSACTIONS OF THE JAPAN SOCIETY OF MECHANICAL ENGINEERS Series B*, 2(480) (1986) 62. ISSN 1884-8346. https://doi.org/10.1299/kikaib.52.2963.

[20] Krivchenko H. *Hydraulic machines: turbines and pumps: A textbook for high schools, altered*. Energoatomizdat, Moscow (1983). URL https://books.google.com.np/books/about/Hydraulic_Machines_Turbines_and_Pumps.html?hl=ms&id=QuNSAAAAMAAJ&redir_esc=y.

[21] Wu J, Shimmei K, Tani K, Niikura K & Sato J, CFD-based design optimization for hydro turbines, *Journal of Fluids Engineering*, 129(2) (2007) 159–168. ISSN 1528-901X. https://doi.org/10.1115/1.2409363.

[22] Quishpe L, Valencia E, Hidalgo V, Zambrano O & Cando E, Evaluation of guide vanes effect over runner Francis turbine sediment erosion using a quasi-two dimensional approach, *IOP Conference Series: Earth and Environmental Science*, 774(1) (2021) 012077. ISSN 1755-1315. https://doi.org/10.1088/1755-1315/774/1/012077.

[23] Wilcox D C et al. *Turbulence modeling for CFD*, vol. 2. DCW industries La Canada, CA (1998). URL https://books.google.ca/books/about/Turbulence_Modeling_for_CFD.html?id=aolIPgAACAAJ&source=kp_book_description&redir_esc=y.

[24] Gubin M F. *Draft tubes of hydro-electric stations*. Amerind Publishing Company for the US Bureau of Reclamation (1973). URL https://www.google.com.np/books/edition/Draft_Tubes_of_Hydro_electric_Stations/ex3dAAAAIAAJ?hl=en&gbpv=0&bsq=drafttubesofhydro.